East European Journal of Physics. **1.** 460-475 (2024)
DOI:10.26565/2312-4334-2024-1-51 ISSN 2312-4334

MECHANISM OF HYDROGEN PRODUCTION IN THE PROCESSES OF RADIATION-HETEROGENEOUS SPLITTING OF WATER WITH THE PRESENCE OF NANO-METAL AND NANO-MeO

Adil Garibov[a], Yadigar Jafarov[a], Gunel Imanova[a,b,c]*, Teymur Agayev[a], Sevinj Bashirova[d], Anar Aliyev[a]

[a] *Institute of Radiation Problems, Ministry of Science and Education Republic of Azerbaijan, 9 B. Vahabzade str., AZ1143, Baku, Azerbaijan*
[b] *UNEC Research Center for Sustainable development and Creen economy named after Nizami Ganjavi, Azerbaijan State University of Economics (UNEC), 6 Istiglaliyyat Str., Baku 1001, Azerbaijan*
[c] *Khazar University, Department of Physics and Electronics, 41 Mahsati Str., AZ1096, Baku, Azerbaijan*
[d] *MDİ NASA of Space Research of Natural Resources, AZ 1115, Baku, S.S. Akhunzade, 1, Azerbaijan*
**Corresponding Author e-mail: radiasiya555@rambler.ru*
Received December 17, 2023; revised January 16, 2024; accepted January 29, 2024

In the study, the optimal values of the ratio of the distance between particles to the particle size in the radiation-heterogeneous radiolysis of water in nano-Me and nano-MeO systems were determined. In those systems, the effect of water density and system temperature on the radiation-chemical release of molecular hydrogen obtained from thermal and radiation-thermal decomposition of water was considered. The article also determined the effect of particle sizes and the type of sample taken on the radiation chemical yield of molecular hydrogen. In the presented article, the change of molecular hydrogen according to adsorbed water and catalyst was studied. Thus, in the case of a suspension of nano-zirconium in water, the energy of electrons emitted from the metal is completely transferred to water molecules, which leads to an increase in the yield of hydrogen. When radiolysis of water in the presence of nano-metals, energy transfer can be carried out mainly with the participation of emitted electrons. Therefore, in the case of radiolysis of water in suspension with n-Zr, the yield of hydrogen increases by 5.4 times compared to the processes of radiolysis in an adsorbed state. However, in radiation-heterogeneous processes of obtaining hydrogen from water in contact with metal systems, it is necessary to take into account that as a result of these processes surface oxidation occurs and after a certain time the systems are converted to n-Me-MeO+$H_2O_{liq.}$ systems. For nano sized oxide compounds, the mean free path of secondary electrons formed as a result of primary processes of interaction of quanta with atoms is commensurate with the particle sizes of nano-oxides ($\lambda \approx R\_(H\text{-}oxides)$). Further, these electrons interact with the electronic subsystem of silicon. For nanocatalysts, the length of free paths of secondary and subsequent generations of electrons is greater than the size of catalyst particles ($R\_cat \leq 100nm$). Usually, their energy is sufficient to conduct independent radiolytic processes in the contact medium of the catalyst.
Keywords: *Nano-Me and nano-MeO oxides; γ-Radiation; Molecular hydrogen generation; Radiolysis; Second electron cloud*
PACS: 541.15:541.183:620.3

INTRODUCTION

Nanosized metal oxide photocatalyst materials for water splitting have emerged as the promising way for hydrogen generation in a low-cost and sustainable way. Various researchers have reported investigations on co-relation of crystallinity and morphology of nanomaterials to the water-splitting performance. In general, the nanomaterials with high surface-to-volume ratios are expected to promote facile charge separation/transportation of photogenerated charge carriers [1-3].

Overall, more work needs to be done in terms of redox material engineering, reactor technology, heliostat cost reduction and gas separation technologies before commercialization of this technology [4].

The yields of molecular hydrogen, H_2, have been measured in the radiolysis of dodecane and hexane following radiolysis by γ-rays and a variety of heavy ions. Increasing the linear energy transfer (LET) from γ-rays to radiolysis with protons results in a decrease of H_2 yields by about 15% due to the increased importance of second-order H atom combination reactions. A further increase in LET results in a slight increase in H_2 yields [5].

The results suggest that the increase in H_2 production is due to the transfer of energy, possibly by an exciton, from the oxide to the water. O_2 production was at least an order of magnitude less than H_2. The yield of H_2 in the 5 MeV helium ion radiolysis of water on CeO_2 is the same as with γ-rays, but the results with ZrO_2 are substantially lower. The H_2 yields with helium ion radiolysis may be nearly independent of the type of oxide [6-10].

The differences in the relative increases in molecular hydrogen with increasing LET for each of the polymers suggests that self-scavenging reactions may be important for low LET particles [11].

It has been revealed that at increase in mass of the silicon added to water the radiation–chemical yield of the molecular hydrogen received in the process of a water radiolysis grows in direct ratio ($m < 0.02$ g) and depending on the sizes of particles after a certain mass value ($m > 0.02$ g) the stationary area is observed. In the Si+H_2O system the maximum radiation-chemical yield of molecular hydrogen is equal to 10.9; 8.07, and 5.24 molecules/100 eV at the sizes of silicon particles d = 50, 100, and 300…500 nm respectively [12].

Cite as: A. Garibov, Y. Jafarov, G. Imanova, T. Agayev, S. Bashirova, A. Aliyev, East Eur. J. Phys. 1, 460 (2024), https://doi.org/10.26565/2312-4334-2024-1-51

The kinetics of molecular hydrogen accumulation at a gamma radiolysis of water on n-ZrO_2 surface is investigated. Influence of gamma radiations on n-ZrO_2+water systems is studied at various temperatures T = 300…673 K [13].

At a temperature of T = 673 K, the yield and the rate of formation of molecular hydrogen obtained in the thermal and radiation-thermal transformation of water vapor in the reaction medium increase in direct proportion to the its density at $\rho < 3$ mg/cm^3, and at $\rho \geq 3$ mg/cm^3 a sharp decrease in the angle slope is observed [14].

It has been established that the amount, formation rate and radiationchemical yield of molecular hydrogen defined according to both water and BeO from radiation-heterogeneous transformation of water in these systems, change depending on mass and particle size of BeO added to water [15].

Different strategies could be implemented to improve the water splitting efficiency of semiconductors. Among them, loading of catalyst onto the water splitting material is known to be one of the effective strategies to enhance the H_2 and O_2 production rates. Conclusively, to explore the efficient catalysts for photochemical water splitting require more research contribution towards the understanding of the core reaction mechanism of catalytic process with the use of sustainable and stable materials [16-17].

In the last years, the awareness of climatic change has increased leading to the temptation of exploration of alternative sources of energy. Consequently, the use of nuclear energy is increasing day by day but it is not economically and environmentally favorable [18]. Transforming nuclear energy into a more affordable form of energy remains one of today's needs. Therefore, the request for green energy is the chief objective for the scientists in 21 century. The significant methods include photocatalytic, photo-electrochemical, thermal decomposition and photo-biological radiolysis. Among these, photocatalytic of water is measured as the best one due to green, efficient, inexpensive with the comfort of process and with a good volume of hydrogen formed [19].

For a long time, dissimilar groups of catalysts are being developed and utilized to split water in the light but a good crop of hydrogen could not be attained at a good scale. Nanocatalysts have been produced and utilized in water splitting with good achievements [20].

Zirconium dioxide (ZrO_2) has unique properties of refractoriness, low volatility, high chemical resistance, mechanical strength, wear resistance, low thermal conductivity, wide band gap, oxygen conductivity, and high refractive index. Also, zirconium dioxide has complex polymorphisms, including high-pressure phases. The unique properties have provided a wide and varied application of materials based on ZrO_2 in various fields of science and technology. Currently, the development of new technologies for the production and obtaining nanodioxide zirconium is of particular importance. Nanoscale systems differ in many respects from ordinary single-crystal systems, therefore, the study of their interaction with water under the influence of γ-radiation is of great practical and scientific interest in the field of high-energy chemistry, as well as in solving environmental problems [21].

The results showed that surface morphology is extremely important in the decomposition of liquids at solid interfaces, which may have many consequences ranging from nuclear waste storage to the H_2 economy. The presented work is devoted to the kinetics and mechanism of the formation of hydrogen as a result of the decomposition of water on the surface of nano-ZrO_2 [22].

METHOD

The experiments were performed at the static condition in specific quartz ampoules, with V = 1.0 cm^3 of volume. In order to prevent oil and lubricants from falling on the samples, three nitrogen-cooled holders are connected to the system in a vacuum-absorption device. The products of the radiolysis and thermoradiolysis of water were absent under the selected treatment modes which can be formed in the presence of organic impurities CO and CO_2. The absorption process was the same for both methods (vapor and fluid). The gases generated were inhaled from each adsorbed ampoule to the chromatograph directly [23].

Analysis of molecular hydrogen and hydrogen-containing gases in a vacuum absorption device was carried out under static conditions. Radiation-heterogeneous processes were performed at the gamma ^{60}Co isotope source. The dosimetry of the source was determined by ferrosulfate, cyclohexane and methane dosimeters [24]. The absorbed dose rate of the source was $dD\gamma/dt = 0.40$ Gy/s. The calculation of the absorption dose in these systems was carried out in comparison with the electron density. The absorption dose of gamma quanta was determined under the methods of ferrosulfate, cyclohexane and methane based on chemical dosimeters in the studied systems.

The ampoules were opened in a special box in which the radiolysis products entered the chromatograph column. The analysis of the products of radiation-heterogeneous processes was performed using “Gasochrome-3101”, “Color-102”, chromatographs.

Analysis of the number of products (H_2, CO_2) gases released in the gas phase during the thermal and radiation-thermal decomposition of water on the nano-Me and nano-MeO+H_2O system was carried out by chromatographic method (“Gasochrome-3101”, “Color-102”, chromatographs). The molar density of gases in 1 mL was calculated by the following equation:

$$C_i = h_i m K_i$$

where: molar density of C_i-i component, molecule/ml or mol/ml; height of h_i-i-th component, mm; m - sensitivity of the chromatograph; Calibration coefficient of the K_i-i component, molecule/mm or mol/mm.

The following formula was used to calculate the substance content of the components obtained in the gas phase during the experiment:

$$N_i = C_i V$$

where: molar mass, molecular or mole of N_i-i component; Molar density of C_i-i component, molecule/ml or mol/ml; V - a volume of the ampoule tested, ml.

The chromatographic analysis of radiation-catalytic products of water decomposition was carried out.

RESULTS AND DISCUSSION

Obtaining molecular hydrogen during radiation-heterogeneous processes in suspensions of individual nano-elements (n-Zr and n-Si) in water. In order to reveal the contribution of secondary electron fluxes emitted from the solid phase in the radiation-catalytic processes of hydrogen production, the kinetics of hydrogen production processes as a result of heterogeneous decomposition of water in the presence of nano-metal (n-Zr) and individual nano-semiconductor n-Si were studied (Fig. 1).

The effect of n-Zr and n-Si on the release of molecular hydrogen during radiolysis of water is investigated in their suspension in water [25]. The kinetics of hydrogen production are investigated and radiation-kinetic outputs and process speeds are calculated based on them.

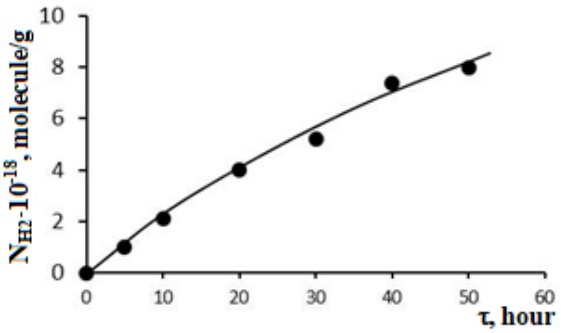

Figure 1. Kinetics of obtaining molecular hydrogen during radiolysis of water in n-Zr+H_2O suspension, at T = 300K, D = 0.15 Gy/s

On the basis of the kinetic curve, the kinetic parameters of hydrogen production are determined

$$W(H_2) = 6.67 \cdot 10^{13} molecules \cdot g^{-1} \cdot s^{-1};\ G_{tot}(H_2) = 7.1\ molecules/100eV \quad (1)$$

During radiation-heterogeneous radiolysis of water in a liquid state in the presence of n-Zr, the yield of molecular hydrogen is approximately 5.5 times greater than during the radiolysis of adsorbed states of water on the surface of n-Zr with a monolayer filling of the surface θ = 1.

Thus, in the case of a suspension of nano-zirconium in water, the energy of electrons emitted from the metal is completely transferred to water molecules, which leads to an increase in the yield of hydrogen. However, in radiation-heterogeneous processes of obtaining hydrogen from water in contact with metal systems, it is necessary to take into account that as a result of these processes surface oxidation occurs and after a certain time the systems are converted to n-Me-MeO+$H_2O_{liq.}$ systems.

Under the influence of γ-quanta on n-Si, secondary electrons are generated with an energy

$$E_H \approx E_g + \Delta E_k, \quad (2)$$

where E_g- is the band gap of the semiconductor, ΔE - k are their additional kinetic energies.

Therefore, in the case of radiation-catalytic decomposition of water in the presence of a nano-semiconductor, for efficient energy transfer, it is necessary to have a condition for the interaction of energy carriers with water molecules. The effect of n-Si on the yield of molecular hydrogen during the radiolysis of water in a suspension of n-Si+$H_2O_{liq.}$ was studied at various $H_2O_{liq.}$/n-Si ratios [26]. To do this, we took 5 ml of bidistilled water and poured n-Si with different particle sizes into it in various amounts. Based on the weight of n-Si in the suspension and particle size, the concentrations of n-Si in V = 5 ml of water were calculated.

For this, the n-Si particles were presented as a sphere and the volume of each particle was determined by the average value of the ball radius (R_i) by $V = \frac{4}{3}\pi R^3$. Taking into account the value of the specific gravity of n-Si (ρ=2.33 g), the mass of each particle $m_{particle}$=V·Q was determined.

The ratio of $m_{n\text{-}Si}$ to the mass of each particle makes it possible to determine the total number of particles in 5 ml of suspension $N_i = \frac{m_{n-Si(R_i)}}{m_{partic.(R_i)}}$ and based on them the concentration is estimated n-Si with different particle sizes $C_{n-Si} = \frac{N_i(R_i)}{V_{suspen.}}$. The values of the mass and concentration of n-Si for each fraction are shown in Table 1.

Under experimental conditions, the mass of $n-Si$ $m_{n-Si} \leq 0.12\ g$ is much less than the mass of water $\frac{m_{H_2O}}{m_{n-Si(max)}} = 42$. Therefore, the observed yields of molecular hydrogen were calculated both on the energy of absorbed ionizing radiation from the side of water $G_{H2O}(H_2)$ and from the side of n-Si $G_{(n\text{-}Si)}$ (H_2). Table 1 shows the values of the radiation-chemical yield of hydrogen during radiation-heterogeneous radiolysis of water in the n-Si + $H_2O_{liq.}$ system at various amounts, concentrations and sizes of the catalyst particle per gamma-radiation energy absorbed from the water side.

With an increase in the concentration of n-Si in water under the influence of gamma rays, the yield of molecular hydrogen increases. Figure 2 (a, b, c) shows the dependences of $G_{H2O}(H_2)$ on the concentration of n-Si with different particle sizes in a suspension of n-Si+$H_2O_{liq.}$

Table 1. Effect of n-Si Concentration during Heterogeneous Radiolysis of Water in the Presence of n-Si (in Suspension)

$n-Si$ R, Gy	$d = 50nm$			$d = 100nm$			$d = 300-500nm$		
	C_{n-Si}, particle/cm^3	$W(H_2)\cdot 10^{-13}$ molekule$\cdot$ g$^{-1}\cdot$s^{-1}	$G_{H_2O}(H_2)$ molecule/ 100eV	C_{n-Si}, particle/cm^3	$W(H_2)\cdot 10^{-13}$ molecule$\cdot$ g$^{-1}\cdot$s^{-1}	$G_{H_2O}(H_2)$ molecule/100eV	C_{n-Si}, particle/cm^3	$W(H_2)\cdot 10^{-13}$ molecule$\cdot$ g$^{-1}\cdot$s^{-1}	$G_{H_2O}(H_2)$ molecule/100eV
0	0	0,61	0,44	0	0,61	0,44	0	0,61	0,44
0.01	$1.32\cdot10^{13}$	5.00	3.64	$1.65\cdot10^{12}$	3.40	2.77	$2.56\cdot10^{10}$	2.53	1.84
0.02	$2.63\cdot10^{13}$	9.67	7.03	$3.3\cdot10^{12}$	7.97	5.48	$5.12\cdot10^{10}$	5.15	3.75
0.06	$7.89\cdot10^{13}$	13.40	9.05	$9.92\cdot10^{12}$	9.67	7.03	$15.36\cdot10^{10}$	6.30	4.58
0.12	$15.73\cdot10^{13}$	15.00	10.90	$12.84\cdot10^{12}$	11.10	8.07	$30.72\cdot10^{10}$	7.21	5.24

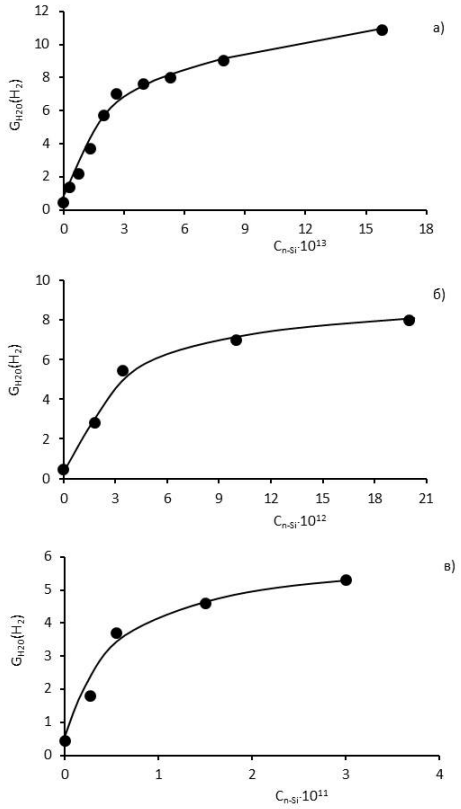

Figure 2. Dependence of $G_{H_2O}(H_2)$ on n-Si concentration in $n-Si+H_2O_{liq.}$ suspension for different particle sizes (a) d = 50nm; (b) d = 100nm; (c) d = 300-500nm, at T = 300K, D = 22 rad/s

As can be seen, the addition of even the smallest amount of n-Si to water causes a sharp increase in the yield of molecular hydrogen during radiation-heterogeneous processes in the n-Si + $H_2O_{liq.}$ system.

Dependence $G_{H_2O}(H_2) = f(C_{n-Si})$ can be conditionally divided into two sections. The first is the initial linear region, where $G_{H_2O}(H_2)$ grows linearly with increasing C_{n-Si}. The second region $G_{H_2O}(H_2) = f(C_{n-Si})$ is characterized by a small slope of the dependence line. If radiation-heterogeneous processes would occur only on the surface of n-Si particles, then the rate and radiation-chemical yields of hydrogen would increase linearly with increasing C_{n-Si}.

The value of C_{n-Si}, at which a transition between these regions is observed, depends on the size of the n-Si particles (Table 2.). For the convenience of calculation for the fraction d=300-500 nm, the average value $\bar{d}$=400 nm was taken.

Table 2. Influence of n-Si concentration and distance between particles during water radiolysis in the $n-Si+H_2O$ system (in suspension)

$\bar{R}_{n-Si}$, nm	G_{H_2O}, molecule/100eV	C_{n-Si}, particle/cm^3	l distance between particles, nm	l , nm	$l_n/d_ч$
25	7.3	$4.0\cdot10^{13}$	l=(60÷1.24)·10^4	$1.89\cdot10^4$	$3.78\cdot10^2$
50	6.5	$6.0\cdot10^{12}$	l=(4.6÷0.1)·10^5	$3.14\cdot10^4$	$3.14\cdot10^2$
200	4.2	$1.0\cdot10^{11}$	l=(18.4÷0.98)·10^5	$1.18\cdot10^5$	$2.95\cdot10^2$

By the value of the number of particles in the suspension and the specific surface of individual spherical particles $S_{particle} = 4\pi R^2$, the surface of the total amount of n-Si is determined in the form

$$S_{tot.} = N_i \cdot S_{particle} \tag{3}$$

where N_i – is the total number of particles in the water.

By the value of ω - the landing area of water on the surface of silica gel ω=0.453 nm^2, the number of water molecules to fill the surface with a monolayer of water is determined

$$N(\theta = 1) = \frac{S_{tot.}}{\omega_{H_2O}} \tag{4}$$

Then the hypothetical value of the number of monolayers was estimated by the number of water molecules in the suspension ($m = 5g$) $N_{H_2O} = 1.72 \cdot 10^{23} molecules$ and $N(\theta = 1)$

$$N(monolayers) = \frac{1.72\cdot10^{23} molecul}{N(\theta=1)} \tag{5}$$

By the value of the hypothetical value of the monolayers filling the surface of n-Si and the diameter of water molecules d(H_2O) = 0.38 nm, one can approximately determine the distance between the particles in the suspension $n-Si+H_2O_{liq}$.

$$l = d_{H_2O} \cdot N(monolayers) \tag{6}$$

The value of the distance between n-Si particles in the suspension was determined both in the entire region of n-Si concentration and at the transition point between the regions of dependences $G_{H_2O}(H_2) = f(C_{n-Si})$.

To characterize the distance of influence of individual n-Si particles on radiation-heterogeneous processes in a suspension, distances l is given per unit of particle diameter l_n/d_{n-Si}.

As can be seen from Table 2, with an increase in the size of the n-Si particle in the H_2O + n-Si suspension, the radiation-chemical yield of hydrogen, calculated for the energy of γ - radiation absorbed from the water side, decreases. It was found that the value of the distance, given per unit of n-Si diameter within the limits of accuracy, is constant $\bar{l}/d \approx 3.3 \cdot 10^2 nm$.

This distance is consistent with the mean free path of secondary electrons with energy $E \approx 10^2 - 10^3$ in water.

To characterize the efficiency of using the energy absorbed from the n-Si side during the radiolysis of water in the $n-Si+H_2O_{liq.}$ suspension, based on the kinetic curves of hydrogen accumulation, the values of the radiation-chemical yield of hydrogen for the absorbed radiation dose from the n-Si side were calculated. Figure 3. shows the dependence of $G_{n-Si}(H_2)$ on the concentration of n-Si in water.

As can be seen, up to the value of the n-Si concentration corresponding to the transition (Table 2) $G_{n-Si}(H_2)$, remains high. Then, a region of strong decline begins with a transition to a region of decrease with a small slope of the curves.

The n-Si particles play the role of converting the energy of primary quanta into the energy of secondary electron radiation. The energy of secondary electron radiation is in the region of $E \leq 10^3 eV$ eV. Figure 3 shows the dependence of the radiation-chemical yield of molecular hydrogen, calculated on the energy absorbed only from the side of $n-Si$ $G_{n-Si}(H_2)$, on the concentration of n-Si with particle sizes d=50nm in suspension. As can be seen, in the initial region

$C_{n-Si} \leq 2.5 \cdot 10^{13} particle/cm^3$, the hydrogen yield in the limit of determination accuracy is stably high $G_{n-Si}(H_2) \approx$ 1700-1780 molecules/100 eV. At optimal concentrations of n-Si in suspension with water, the observed yields of hydrogen exceed the value of the yield during radiolysis of water under the action of γ-radiation and accelerated electrons [27].

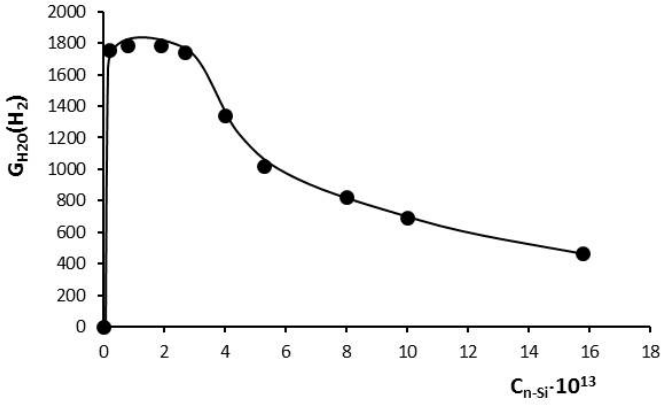

Figure 3. Dependence of $G_{n-Si}(H_2)$ during radiolysis of water in n-Si suspension with d = 50 nm in water on n-Si concentration, T = 300K, $\dot{D} = 22\ Rad/s$.

Apparently, at the initial values of the concentration $C_{n-Si} \leq C_{n-Si}$ (transition), a region with a high electron density is created around the particle, and the decomposition of water molecules occurs according to the mechanism of decomposition of water in a nonequilibrium plasma [28]. An increase in the concentration of $C_{n-Si} \geq 2.5 \cdot 10^{13}$particles/cm^3 causes a decrease in the yield of $G_{n-Si}(H_2)$ from 1780 to 430 molecules/100 eV at $C_{n-Si} = 15.8 \cdot 10^{13}$ particles/cm^3. The observed dependences of $G_{n-Si}(H_2)$ and $G_{n-Si}(H_2)$ on C_{n-Si} in suspension show that after certain values of C_{n-Si} radiation processes occur, which cause a decrease in the conversion efficiency energy of ionizing radiation into the energy of hydrogen. Therefore, after C_{n-Si} (transition), the growth rate of $G_{H_2O}(H_2)$ decreases, and $G_{n-Si}(H_2)$ sharply decreases.

Based on the results obtained on the effect of the n-Si concentration in water on the yield of molecular hydrogen during water radiolysis, it can be concluded that the optimal range of n-Si concentration values for efficient conversion of ionizing radiation energy into hydrogen energy. Since at values $l/d \geq 3 \cdot 10^{-2}$ there is an efficient conversion of the energy of ionizing radiation into the energy of hydrogen. In the region $l/d \leq 3 \cdot 10^{-2}$, at which the distance between the particles related to the size unit n-Si decreases, the recombination of charged and intermediate decomposition products of water molecules increases.

The maximum yield of hydrogen during radiolysis of water in an n-Si suspension under the optimal regime corresponds to $G_{H_2O}(H_2)$ = 10.9 molecules/100eV. The efficiency of converting the energy of ionizing radiation into relative conditions is

$$\eta = 2.96G(H_2) = 32.3\ \%. \tag{7}$$

And during the radiolysis of water in suspension with $n - ZrO_2$, the yield of molecular hydrogen calculated for the energy absorbed by the total system $-ZrO_2 + H_2O_{ж}$ равно $G_{tot.}(H_2) = 13.5\ molecule/100eV$.

The efficiency of converting the energy of ionizing radiation will be equal to

$$\eta = 2.97G_{tot.}(H_2) \approx 39.96\ \%. \tag{8}$$

Radiation-thermal processes of hydrogen production from water in the presence of nano-oxide compounds. Thermo-radiation processes for producing hydrogen are designed to convert the energy of high-temperature reactor models. As can be seen, an increase in temperature during radiation-thermal-catalytic processes stimulates the diffusion of energy carriers on the surface and secondary processes of transformation of intermediate products to final products. For nano sized oxide compounds, the mean free path of secondary electrons formed as a result of primary processes of interaction of quanta with atoms is commensurate with the particle sizes of nano-oxides ($\lambda \approx R_{H-oxides}$). Therefore, temperature will most of all affect the secondary physicochemical and chemical processes of heterogeneous water radiolysis. Thermal and radiation heterogeneous processes were carried out under the same conditions [29]. Kinetic parameters of thermocatalytic and radiation-thermocatalytic processes are determined on the basis of kinetic curves. The rate of radiation-catalytic processes of hydrogen production is determined by the difference in the values of experimentally determined radiation-thermal catalytic $W_{PT}(H_2)$ and $W_T(H_2)$ thermocatalytic processes.

$$W_R(H_2) = W_{RT}(H_2) - W_T(H_2) \tag{9}$$

Based on the values of $W_R(H_2)$, the values of the radiation-chemical yields of hydrogen ($G(H_2) = W \cdot J^{-1} \cdot 10^2$) were calculated. $n - SiO_2$, $n - Al_2O_3$ and $n - ZrO_2$ were taken as the object of research.

Their physicochemical properties are given in the previous sections. Figure 4 shows typical forms of kinetic curves for hydrogen production in the results of thermocatalytic (1) and radiation-thermocatalytic (2) decomposition of water at T = 673 K in the presence of $n - ZrO_2$.

The effect of temperature on the radiation-catalytic properties of nano-oxides was studied in the temperature range T = 300÷673 K at the water vapor density in the reactor $\rho = 5mG/cm^3$.

Table 3 shows the rates of radiation-thermal, thermal and radiation processes, as well as radiation-chemical yields of hydrogen, calculated for the energy absorbed by the common catalyst system+H_2O.

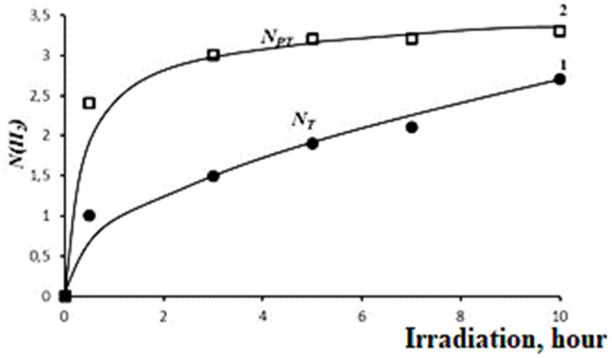

Figure 4. Kinetic curves for the production of molecular hydrogen during thermocatalytic (1) and radiation-thermocatalytic (2) decomposition of water in the presence of n$-ZrO_2$, $d = 20 - 30nm, T = 673K, \rho_{H_2O} = 5mG/cm^3, \dot{D} = 0.26g/s$

Table 3. The value of the rates of processes and radiation-chemical yields of hydrogen during thermal and radiation-thermal catalytic processes of water decomposition in the presence of n-ZrO_2 at different temperatures

№	T, K	$W_i(H_2) \cdot 10^{-14} molecule/g \cdot s$			$G_{tot}(H_2)$, $molecule/100eV$
		$W_{RT}(H_2)$	$W_T(H_2)$	$W_R(H_2)$	
1	300	-	-	0,44	2,14
2	373	0.91	0.13	0.78	4.80
3	423	1.67	0.44	1.23	6.20
4	473	2.08	0.55	1.52	8.35
5	573	3.33	1.11	2.22	13.60
6	673	6.94	2.78	4.16	25.70

The corresponding methods determined the values of the rates of processes and radiation-chemical yields of hydrogen during radiation-thermal processes of water decomposition in the temperature range T = 300÷673K in the presence of, n$-Al_2O_3$ and $n - SiO_2$.

The results obtained are shown in Tables 4 and 5.

Table 4. Influence of temperature on thermo- and radiation-thermal catalytic processes of obtaining molecular hydrogen in the system n$-Al_2O_3 + H_2O$, $\rho_{H_2O} = 5mG/sm^3$

№	T, K	$\dot{D}$, Gy/s	$W_i(H_2) \cdot 10^{-13} molecule/g \cdot s$			$G_{tot}(H_2)$, $molecule/100eV$
			$W_{RT}(H_2)$	$W_T(H_2)$	$W_R(H_2)$	
1	300	0.26	-	-	$3.10 \cdot 10^{13}$	1.75
2	373	0.14	$2.78 \cdot 10^{13}$	$0.69 \cdot 10^{13}$	$2.09 \cdot 10^{13}$	2.75
3	473	0.14	$5.83 \cdot 10^{13}$	$2.22 \cdot 10^{13}$	$3.61 \cdot 10^{13}$	4.15
4	673	0.13	$9.44 \cdot 10^{13}$	$4.17 \cdot 10^{13}$	$5.27 \cdot 10^{13}$	8.60

Table 5. Influence of temperature on thermo- and radiation-thermal catalytic processes of obtaining molecular hydrogen in the system n$-SiO_2 + H_2O$, $\rho_{H_2O} = 5mG/sm^3$

№	T, K	$\dot{D}$, Gy/s	$W_i(H_2) \cdot 10^{-13} molecule/g \cdot s$			$G_{tot}(H_2)$, $molecule/100eV$
			$W_{RT}(H_2)$	$W_T(H_2)$	$W_R(H_2)$	
1	300	0.20	-	-	$0.89 \cdot 10^{12}$	0.61
2	373	0.11	$0.86 \cdot 10^{13}$	$0.12 \cdot 10^{13}$	$0.74 \cdot 10^{13}$	1.07
3	473	0.11	$2.70 \cdot 10^{13}$	$0.99 \cdot 10^{13}$	$1.71 \cdot 10^{13}$	1.98
4	673	0.11	$5.23 \cdot 10^{13}$	$2.4 \cdot 10^{13}$	$2.83 \cdot 10^{13}$	4.15

As can be seen n-ZrO_2 exhibits a relatively high radiation-thermal catalytic activity. At T = 673K, the observed value of the radiation-chemical yield of molecular hydrogen during radiolysis of water in the presence of $n-ZrO_2$ is equal to $G_{tot}\,(H_2) = 25.7 molecul/100eV$. The process of thermo-radiolysis of water occurs in the gaseous state, and therefore the efficiency of the energy conversion process in this system is

$$\eta(H_2) = 2.51 G_{tot.}(H_2) = 64.51\ \%. \tag{10}$$

Thus, radiation-thermocatalytic processes of hydrogen production from water at T ≥ 673K can compete with electrolysis processes in terms of efficiency.

Radiolytic decomposition of water molecules at T≥673K in the presence of $n-ZrO_2$ can occur both with the participation of energy carriers at the surface levels and with secondary electron radiation from $n-ZrO_2$ in the gas phase. The band gap width of $n-ZrO_2$ can be taken as $E_g = 5.4$ eV and the yield of such energy carriers as an electron and a hole will be equal to

$$G = \frac{100eV}{2E_g} \approx 9\ vapor/100eV. \tag{11}$$

At T ≥ 673K, the intermediate H atoms are transformed into H_2 according to reaction (11).

$$H + H_2O \rightarrow H_2 + OH \tag{12}$$

Therefore, the output of molecular hydrogen as a result of radiolysis of water with the participation of non-equilibrium charge carriers formed under the action of ionizing radiation will correspond to $G_{tot.}(H_2) = 9\ molecule/100eV$.

On the other hand, excitons are also generated in $n-ZrO_2$under the action of γ-quanta, which can participate in the process of energy transfer. The size of the investigated samples of $n-ZrO_2$ varies in the region d = 20-30 nm, which is less than the mean free path of secondary electrons λ ≥ 2R and it can be expected that a certain part of the electrons will be emitted into the contact medium with $n-ZrO_2$. Ultimately, these energy transfer channels from $n-ZrO_2$ in water can provide the observed value of the hydrogen yield.

Influence of temperature on the output of molecular hydrogen during radiolysis of water in the presence of n-Zr and n-Si. When radiolysis of water in the presence of nano-metals, energy transfer can be carried out mainly with the participation of emitted electrons. Therefore, in the case of radiolysis of water in suspension with n-Zr, the yield of hydrogen increases by 5.4 times compared to the processes of radiolysis in an adsorbed state. Based on the results of the radiation-thermocatalytic processes of hydrogen production from water presented in the previous sections, it is possible to conclude that their speed depends on the following parameters of the process regime.

$$W_{RT}(H_2) = f\left(T, \dot{D}, \rho_{H_2O}, S/V, LET\ \right), \tag{13}$$

where is the temperature, $\dot{D}$-radiation, LET-linear radiation energy transfer, ρ_{H_2O} is the density or pressure of water vapor in the reaction medium, S/V dispersion of microsized or particle size of nanosized solids.

In order to reveal the regularities of the effect of temperature on the yield of molecular hydrogen, the kinetics of water radiolysis in the presence of n-Zr was studied in the temperature range T = 300÷673K, at a water vapor density in the reaction medium ρ_{H_2O} = 5mg/cm^3 and power exposure doses $\dot{D}$ = 0.32÷0.26 Gy/s [30]. The values of the rates of the processes and the radiation-chemical yield of molecular hydrogen are given in Table 6.

Table 6. The value of the rates of thermo-, radiation-thermal and radiation-catalytic processes in the n-Zr+H_2O contact and the radiation-chemical release of hydrogen in the temperature range, T= $300 \div 673K$, $\rho_{H_2O} = 5mG/cm^3$, $\dot{D} = 0.32 \div 0.26 Gy/s$

№	*T, K*	$W_{RT}(H_2)$, $molecule/g \cdot s$	$W_T(H_2)$, $molecule/g \cdot s$	$W_R(H_2)$, $molecule/g \cdot s$	$G_{tot}\,(H_2)$, $molecule/100eV$
1	300	-	-	$1{,}22 \cdot 10^{13}$	1,30
2	373	$4.10 \cdot 10^{13}$	$2.60 \cdot 10^{13}$	$1.50 \cdot 10^{13}$	2.10
3	473	$5.56 \cdot 10^{13}$	$2.77 \cdot 10^{13}$	$2.79 \cdot 10^{13}$	3.70
4	573	$8.88 \cdot 10^{13}$	$5.00 \cdot 10^{13}$	$3.88 \cdot 10^{13}$	5.20
5	673	$1.33 \cdot 10^{14}$	$0.70 \cdot 10^{14}$	$0.63 \cdot 10^{14}$	8.40

The value of the activation energy of the processes of thermo-heterogeneous and radiation-thermal processes on the basis of the dependencies $\ln W_i\,(H_2) \geq f\left(\frac{1}{T}\right)$ was determined to be 33.8 and 22.3 kJ/mol, respectively [30].

The value of $G_{tot.}(H_2)$ during radiation-thermal decomposition of water at T = 673K, $G_{tot.}(H_2) =$ 8.4 molecules/100eV does not differ much from the values of hydrogen yield during radiolysis of water in n-Zr

suspension $G_{tot.}(H_2)$ =7.1 molecules/100eV. The observed difference in the values of the hydrogen yield can be explained by the course of process (12).

The efficiency of converting the energy of ionizing radiation into the energy of hydrogen in radiation-thermal catalytic processes at T = 673K in the gaseous state in the presence of nano-zirconium is equal to

$$\eta = 2.51G(H_2) = 21\ \%. \quad (14)$$

The authors [31-32] studied the effect of temperature on thermal processes, radiation-thermal processes in the $n - Si + H_2O$ contact at various temperatures T = 300÷673K and water vapor density ρ_{H_2O} = 5mg/cm^3.

The effect of water vapor density on the value of kinetic parameters of heterogeneous processes of water decomposition was studied at T = 673 K, $\rho_{H_2O} = 0.25 \div 8$ mg/cm^3 in the presence of n-Si with particle size d = 50 nm. The research results are shown in Table 7.

Table 7. The value of the rates of thermo-heterogeneous, radiation-thermal and radiation-chemical processes, the production of hydrogen in the n-Zr+H_2O system at the size of the n-Si particle d = 50nm and at the temperature T = 673K at the density of water vapor in the reaction medium $\rho_{H_2O} = 0.25 \div 8\ mG/cm^3$

№	$\rho, mG/cm^3$	$W_{RT}(H_2)$, $molecule/g \cdot s$	$W_T(H_2)$, $molecule/g \cdot s$	$W_R(H_2)$, molecule$/g \cdot s$	$G_{tot}(H_2)$, $molecule/100eV$
1	0.25	$1.68 \cdot 10^{14}$	$1.73 \cdot 10^{14}$	$0.05 \cdot 10^{14}$	0.45
2	0.5	$3.34 \cdot 10^{14}$	$3.45 \cdot 10^{14}$	$0.10 \cdot 10^{14}$	0.89
3	1.0	$6.49 \cdot 10^{14}$	$6.70 \cdot 10^{14}$	$0.21 \cdot 10^{14}$	1.85
4	3	$18.74 \cdot 10^{14}$	$19.15 \cdot 10^{14}$	$0.41 \cdot 10^{14}$	3.60
5	8	$20.10 \cdot 10^{14}$	$20.60 \cdot 10^{14}$	$0.50 \cdot 10^{14}$	4.40

At a constant value of water vapor density ρ_{H_2O}, d_к is the catalyst particle size, $\dot{D}$ is the radiation power and LET in (14), the effect of temperature in the region T=300÷673K on the velocities and $G_{tot.}(H_2)$ at thermo-radiolysis of water in the $n - Si + H_2O$ system. The observed research results are shown in Table 8.

Table 8. Effect of temperature on the kinetic parameters of hydrogen production during thermo-radiolysis of water in the presence of n-Si with d = 50nm, ρ_{H_2O}=8 mg/cm^3 under the action of gamma radiation with $\dot{D}$ = 0.18 Gy/s

№	$\rho, mG/cm^3$	$W_{RT}(H_2)$, $molecule/g \cdot s$	$W_T(H_2)$, $molecule/g \cdot s$	$W_R(H_2)$, molecule$/g \cdot s$	$G_{tot}(H_2)$, $molecule/100eV$
1	300	-	$0.32 \cdot 10^{14}$	$0.32 \cdot 10^{14}$	2.87
2	373	-	$0.33 \cdot 10^{14}$	$0.33 \cdot 10^{14}$	2.90
3	473	-	$0.36 \cdot 10^{14}$	$0.36 \cdot 10^{14}$	3.20
4	573	$2.40 \cdot 10^{14}$	$2.88 \cdot 10^{14}$	$0.48 \cdot 10^{14}$	4.20
5	623	$7.22 \cdot 10^{14}$	$7.71 \cdot 10^{14}$	$0.49 \cdot 10^{14}$	4.32
6	673	$2.01 \cdot 10^{15}$	$2.06 \cdot 10^{14}$	$0.50 \cdot 10^{14}$	4.40

The activation energies of thermal and radiation-thermal processes of hydrogen production in the $n - Si + H_2O$ system is determined based on the temperature dependences of the process rates in the Arrhenius coordinates $\ln W_i(H_2) = f\left(\frac{1}{T}\right)$. It was found that in the temperature range T=300÷473K, the radiolysis of water in the presence of n-Si occurs only as a result of radiation-heterogeneous decomposition of water with E = 1.07 kJ/mol. As can be seen from Table 8, in the temperature range T = 573÷673K in the $n - Si + H_2O$ system, thermo-heterogeneous and radiation-thermo-heterogeneous processes of water decomposition are observed. The activation energies of these processes are 68.60 and 53.83 kJ/mol, respectively. Comparison of the activation energies of the processes $W_P(H_2)$, $W_{PT}(H_2)$ and $W_T(H_2)$ shows that radiation processes in the $n - Si + H_2O$ system cause a decrease in the activation energy of the water decomposition process [33-35].

After radiation-heterogeneous processes, oxide phases, hydrides (ZrH_x, SiH_x), hydroxyl groups Zr-OH, Si-OH are formed on the surface. SEM and IR spectrometry methods reveal oxide phases on the surface of the initial n-Zr and n-Si samples. Therefore, radiation-heterogeneous processes of water decomposition actually occur in the contact $n - Si - SiO_2 + H_2O$, $n - Zr - ZrO_2 + H_2O$. As can be seen from tables 7 and 8, n-ZrO_2 have a relatively high radiation-catalytic activity in the process of water decomposition. Therefore, during radiation-thermocatalytic processes of hydrogen production in the $n - Zr - ZrO_2 + H_2O$ system, high yields of molecular hydrogen are observed relative to $n - Si + H_2O$ systems. The values of radiation-chemical yields of hydrogen during thermoradiolysis of water in the systems $n - SiO_2 + H_2O$ and $n - Si + H_2O$ in the temperature range T ≥ 573 K are comparable and vary in the range of 4.15-4.40 molecules/100eV. Therefore, radiolysis and thermo-radiolysis processes in the $n - Zr - ZrO_2 + H_2O$ and $n - Si + H_2O$ systems can be used as model systems for revealing the patterns of energy transfer and surface radiation-chemical processes.

The Mechanism of Radiation-Catalytic Processes for Hydrogen Production from Water

When ionizing radiation interacts with nano-catalysts, primary processes generate free secondary electron radiation, electrons in the conduction band, holes in the valence band, and excitons:

$$nano - cat. \xrightarrow{ion.radiation} e_v + e_{pr} + p + ex \tag{15}$$

In the scheme (15), e_v -are secondary electrons, e_{pr} - are electrons in the conduction band, p-holes in the valence band, ex-excitons, which are formed as the end product of a cascade of processes of interaction of secondary elements with catalyst atoms. As an example, let's look at the physical stage of processes occurring in the $n - Si + H_2O$ system under the action of gamma - quanta with energy $\bar{E}$ = 1.25 MeV [12-15].

It is revealed that the interaction of gamma-quanta with the atoms of the systems occurs mainly according to the mechanism of Compton scattering. With Compton scattering of gamma-quanta from silicon atoms, depending on the scattering angle, the kinetic energy of Compton electrons varies in the range of 0 ... 1.02 MeV. For nanocatalysts, the length of free paths of secondary and subsequent generations of electrons is greater than the size of catalyst particles (R_cat ≤ 100nm). Therefore, in scheme (1), secondary electrons for radiation-heterogeneous processes involving nanoscale catalysts are also indicated as end products.

The physical stage of radiation-heterogeneous processes proceeds for $\tau \leq 1fs$ (femtoseconds) and as a result, ionization (e, p, H_2O^*), excitation ex, H_2O^*) and generation of high-energy electrons [20] occur according to the scheme (15).

Water on the surface of oxide systems creates electron-donor complexes H_2Os, which capture holes formed under the action of ionizing radiation (16). Many radiation catalytic active oxide compounds have broad valence levels, and therefore the holes in them are highly mobile. In the presence of levels of water molecules on the surface, they interact according to the reaction:

$$\oplus + H_2O_s \rightarrow H_2O_s^+ \tag{16}$$

Electrons formed in radiation-catalytically active oxides under the action of ionizing radiation can have energies in a wide range and enter into multiple interactions with the electronic structures of oxides. As a result, they go through approximately the following energy stages.

1. The electron energy becomes less than the ionization energy of the medium $E_e^1 \leq W(I)$, where W(I) is the threshold energy, of the formation of ion vapors in the medium. The value of E_e^1 is the dependence of the band gap for radiation-catalytically active catalysts and is equal to $E_e^1 \approx 2 \div 3\ E_g$ [20]. Taking into account the values of the water ionization potential for W(I) ≈ 30 eV, these electrons can be characterized as underionization electrons. Electrons with energy $E_e^1 \leq W(I)$ in a medium can enter into an electron-electron interaction and generate an excited state of excitons. After certain energies, the electrons are localized in the structural centers and eventually thermolyzed. Exciton levels of radiation catalytic active oxides $E_{ex} \approx E_g - \sigma E$.
2. The value of E_g in radiation catalytic active catalysts varies in the range of 5÷10 eV [21]. And therefore, the localized exciton levels of these oxides are smaller than the values of the band gap and vary in the range $E_{ex} \sim 5 - 8$ eV [22]. For example, in SiO_2 the energy of underexcitation electrons is equal to E ~ 7.4 eV.
3. After the generation of excitons in oxide systems, underexcitation electrons appear, which have a lower E_{ex} ($E_{II}^1 \leq 10\ eV$). These electrons first interact with LO photons and then with acoustic phonons.

In oxide systems, electrons with energies below the ionization threshold W_i can create excitons and enter into an electron-phonon interaction. The electron-phonon interaction is more probable in the electron energy range 4÷20 eV [66]. The electron-phonon interaction occurs first with LO photons and then with acoustic phonons. After numerous collisions, thermalization of electrons occurs. For example, in SiO_2 electrons with an energy of 1÷8 eV, the thermalization time varies in the range $\tau \leq 1fs$ [28]. On average, electrons with energy $E_э \leq W_2(I)$ are thermalized in time τ = 250÷350 fs. The thermalization time of electrons with energy $E_э \leq W_2(I)$ in water is comparable to the thermalization time in SiO_2, which approximately vary in the range τ = 250÷350fs. During thermalization, electrons in both phases in $SiO_2 - H_2O$ systems can move at a distance of several nanometers. For example, for pure SiO_2, electrons with an energy of 3 eV during thermalization can migrate from 8 to 30 nm distances. Table 9 shows the values of relative permittivity (ε_0), onsager radius ($R_0 = q^2/(4\pi\varepsilon_0 k_B T)$), diffusion constant $D = \mu k_B T/q$ and recombination constant of electron with cations (holes) $\gamma = R_0/(4Dt)^{\frac{1}{2}}$: where, q - charge, k_B - Boltzmann constant, T - temperature, μ - particle mobility, t - time [25].

Table 9. The value of the parameters of processes involving nonequilibrium carriers in SiO_2 and H_2O charges

$SiO_2 - H_2O$	ε_0	$R_0(nm)$	$D(nm^2 \cdot s^{-1})$	γ
H_2O	78	0.72	$1.4 \cdot 10^{13}$	0.2
SiO_2	3.9	14.0	$0.5\text{-}3.0 \cdot 10^{14}$	0.8

As can be seen, the values of the electron-hole recombination constants in SiO_2 are 4 times greater than in water. The on sager radius is about 20 times smaller than in SiO_2. And therefore, in water, secondary electrons can propagate a large distance from the parent ion.

Thus, by analyzing the processes occurring in $E_э \leq W_2$ radiation-catalytic active oxides, one can imagine the mechanism of radiation-heterogeneous processes of water decomposition with the participation of energy carriers according to scheme (15).

Formed according to the scheme H_2O^* interacts with electrons from the conduction band:

$$e + H_2O_s^+ \rightarrow H_2O_3^* \tag{17}$$

$H_2O_s^*$ singlet-excited water molecules in the $A'B$ state (E=8.4eV) undergo decay [13]:

$$H_2O_3^* \rightarrow H + OH \tag{18}$$

However, during the recombination of H_2O_s ions with quasi-free electrons, the energy corresponding to dissociative recombination with E ≈ 11 eV is released:

$$e + H_2O_s \rightarrow H_2O_3^* \rightarrow H_2 + OH \tag{19}$$

During the radiation-catalytic decomposition of water in the presence of nanocatalysts at T ≥ 673K, the transformation of H atoms into H_2 can occur according to the reaction [15]:

$$H + H_2O \rightarrow H_2 + OH \tag{20}$$

The radiolysis of water on the surface of oxide systems can involve subexcited electrons formed in the oxide phase [16-18]:

$$e_{subexcited} + H_2O_s \rightarrow H^- + HO\cdot \tag{21}$$

$$H^- + H_2O \rightarrow H_2 + OH^- \tag{22}$$

The course of these reactions was confirmed by the authors as a result of a study of the dissociative capture of electrons with energy $E_e \leq 12$ eV [12]. According to reaction (17) - (22), the maximum yield is observed at the electron energy $E_e = 7.4$ eV.

As is known, during the radiation-catalytic decomposition of water into a surface-adsorbed state, the maximum yield of hydrogen is limited by the total yields of nonequilibrium charge carriers and excitons and is equal to $G(H_2)$~8-9 molecules/100eV. A particularly high yield of molecular hydrogen is observed during the radiolysis of water in suspension with nano-oxides [24-26] and nanosized individual elements Ze, Si [27]. The observed yield of hydrogen in these processes cannot be explained within the framework of the existing theoretical concepts of energy transfer in radiation-heterogeneous processes.

First, it is necessary to analyze the processes of the physical and physical-chemical stages in individual components of H_2O+nanocatalysts. Under the influence of gamma-quanta and electrons on water, the yield of electron-ion pairs is 3.4 vapor/100 eV [32]. Radiation-catalytically active catalysts in terms of electrical properties can be attributed to insulators Eg~4÷9 eV ($nZrO_2$, $nSiO_2$, nAl_2O_3) and n-Si semiconductors with Eg ≈ 1.5 eV. The threshold energies of the formation of electron-hole pairs in them are equal to En (dielectric)=2.0 Eg; En (semiconductor) = 3.0 Eg and the yields of electron-hole pairs when exposed to quanta are 12.5-5.5 vapor/100eV for dielectrics, 22vapor/100eV for semiconductors. On the other hand, the density of solids is greater than that of water. For these reasons, when γ-quanta are exposed to the system of nanocatalysts +H_2O, the concentration of secondary electrons in the solid phase will be much higher than in water. For example, in the n-Si+H_2O system, the number of electron-hole pairs inside a silicon particle is about 18 times greater than in pure water [30].

Individual particles of nanocatalysts can be represented as a sphere with radius R. The mean free path of energy carriers inside this sphere is λ. Effective energy transfer to the surface of the contacting medium can occur if $\lambda \geq R$. Therefore, with a decrease in the particle size of nanocatalysts, the yield of molecular hydrogen during the radiation-catalytic decomposition of water increases [31].

As the energy of secondary electrons increases, the mean free path in dielectrics and semiconductors decreases [56]. Therefore, in the field of action of γ radiation on nanocatalysts, the energy of electrons emitted from them is low and usually lies in the range $\leq 10^2$ eV. The maximum free path of electrons with an energy of 100 eV in water corresponds to 20 nm [33]. Therefore, it can be imagined that during radiation-catalytic processes with the participation of nanocatalysts, a spherical shell with a radius of 20 nm with a high concentration of electrons with energy $E \ll 10^2$ eV is formed around a spherical particle of catalysts with a radius R.

In the reactor of radiation-catalytic processes, nano-particles are in the form of densely packed spheres. Many physical properties of adsorbed water molecules, such as ionization potential, ion formation energy, excited states, and dissociation energy, differ greatly from those of pure water [35]. Therefore, the yields of target products in the radiation-catalytic decomposition of water, depending on the layer of adsorbed states, differ greatly [21-24]. Secondary electron radiation emitted from nanocatalysts after a multiple cascade of processes of electron-electron interactions cause ionization, excitation in the water phase in the volume between nanoparticles and finally become underexcitation electrons ($E < 7.4\ eV$):

$$H_2O \overset{e}{\rightarrow} H_2O^+ + e + e \tag{23}$$

$$H_2O^+ \overset{e}{\rightarrow} H_2O^* \tag{24}$$

The resulting H_2O^+ ions can recombine with electrons, forming H_2O^*:

$$H_2O^+ + e \rightarrow H_2O^* \tag{25}$$

Excited water molecules can decompose according to the reaction:

$$H_2O^* \rightarrow H + OH \tag{26}$$

After multiple electron-electron, electron-phonon interactions during the time $\tau = 10^{-15} - 10^{-12}$ s, electrons can be solvated:

$$e^- + H_2O \rightarrow e_{aq}^- \tag{27}$$

With the participation of e_{aq}^-- in an aqueous medium, the formation of hydrogen can occur according to the following reactions [25-30]:

$$e_{aq}^- + e_{aq}^-(+2H_2O) \rightarrow H_2 + 2OH^- \tag{28}$$

$$k_1 = 5{,}5 \cdot 10^9 m^{-1}\mathrm{c}^{-1}$$

$$e_{aq}^- + H(+H_2O) \rightarrow H_2 + OH^- \tag{29}$$

$$k_2 = 2{,}5 \cdot 10^9 m^{-1}s^{-1}$$

$$H + H \rightarrow H_2 \tag{30}$$

$$k_3 = 7{,}8 \cdot 10^9 m^{-1}s^{-1}$$

However, as a result of these processes, the yield of molecular hydrogen does not exceed the yield of molecular hydrogen during the radiolysis of water under the action of electrons [60-65]. Radiation-catalytic processes of water decomposition in the presence of nano-semiconductor and nano-metal cannot be explained by the above mechanisms of energy transfer in adsorbed water molecules. During the radiolysis of water in contact with metals, the observed high yields of molecular hydrogen are explained by the decomposition of water with the participation of secondary electron radiation emitted from the metal [66].

In the volume between the grains of nanocatalysts during the radiation-catalytic decomposition of water, electrons enter from all sides, forming a volume with a high concentration of electrons (n_e). Approximately, this volume of water can be represented as a sphere with a radius of 20 nm. In this volume $= \frac{4}{3}\pi R^3 = 3.35 \cdot 10^{-17} cm^3$ under normal conditions there will be $n \sim 10^7$ water molecules. If we take into account that the number of gamma quanta falling per unit time and the number of secondary electrons formed as a result of scattering of primary quanta and secondary electrons, we can be sure that in the volume between nanoparticles without a concentration of secondary electrons there will be a high value of the ratios $n_e/[H_2O]$will be quite high. Therefore, the mechanism of one-stage nonequilibrium discharges can be applied [67].

Under excited electrons can expend their energy on vibrational excitation of water molecules and enter into a dissociative attachment reaction with a water molecule. Under excitation electrons lose their excess energy in $\sim 10^{-13}$ s and then thermalize or solvate [56].

The maximum of the dissociative attachment cross section occurs at the electron energy $E_e \approx 6$ eV:

$$e + H_2O \rightarrow H^- + OH \tag{31}$$

In the electron energy range Ee ~ 1-30 eV, multiple dissociative attachment of electrons can occur:

$$e + H^- \rightarrow H + e + e \tag{32}$$

Multiple use of the electron is possible due to the high-rate $K_e = 10^{-6} cm^3/s$ of the destruction of the negative ion H^- by electron impact according to reaction (23-32).

It has been established that at low electron energies (Te ≈ 1eV), the electron energy is spent on vibrational excitation of water molecules. The characteristic vibrational quantum of water molecules is equal to $\hbar\omega = 0.2$ eV. Sequential vibrational excitation of water molecules occurs in the reaction medium, as a result of which highly excited states are populated into vibrational V-V relaxation, and at the end, a reaction occurs with the participation of H_2O^* [57]:

$$H_2O^* + H_2O \rightarrow H + OH + H_2O \tag{33}$$

The rate of this process is expressed with the formula:

$$v_0 = k_0[H_2O]^2 exp[-D(H_2O)/T_v] \tag{34}$$

where $k_0 = 3 \cdot 10^{-10} cm^3/s$ is the collision constant; $D(H_2O)$ =5 eV – water dissociation energy, T_v – vibrational water temperature.

The resulting H and OH radicals carry out chain processes involving vibrationally excited molecules:

$$H + H_2O^* \rightarrow H_2 + OH; \tag{35}$$

$$\Delta H = 15kcal/mol, E_{a_1} = 21kcal/mol$$

$$OH + H_2O^* \rightarrow H + H_2O_2; \tag{36}$$

$$\Delta H = 61kcal/mol, E_{a_2} = 70kcal/mol$$

Chain termination occurs as a result of three-body recombination:

$$H + OH + H_2O \rightarrow H_2O + H_2O; \tag{37}$$

$$k_3 = 3 \cdot 10^{-31} cm^6/s$$

A parallel chain propagation channel can occur in the reaction medium:

$$OH + H_2O^* \rightarrow H_2 + HO_2; \tag{38}$$

$$\Delta H = 51kcal/mol, E_a = 75kcal/mol$$

$$HO_2 + H_2O^* \rightarrow H_2O_2 + OH; \tag{39}$$

$$E_a = 30kcal/mol$$

However, these reactions are inferior to reactions (33) - (39) due to the high activation barrier. At high temperatures T ≥ 673K, H atoms are transformed into H_2 according to the reaction [65]:

$$H + H_2O \rightarrow H_2 + OH \tag{40}$$

As a result of these processes, the yield of molecular hydrogen is doubled.

If we assume that the chain decomposition of water in radiation-catalytic processes with the participation of nanocatalysts begins with the participation of non-equilibrium charge carriers and excitons formed under the action of ionizing radiation on the catalysts ex, the initial outputs are equal

$G_{a.c} = G_{ex} + G_{n.n} = 8\ particle/100eV$. Using these approximate values, you can estimate the length of the chain of hydrogen production processes by the expression:

$$\gamma = \frac{G(H_2)}{G_{a.c.}} \tag{41}$$

During radiation-catalytic processes of water decomposition at T ≥ 673K in the presence of microsized oxide catalysts:

$$\gamma = \frac{G(H_2)}{G_{a.c.}} \tag{42}$$

In the case of the presence of nanosized catalysts $G(H_2)$ ~ 14-26 molecules/100eV and the chain length:

$$\gamma = 1.75 \div 3.75 \tag{43}$$

Thus, in the process of hydrogen production during the radiation-catalytic decomposition of water in the presence of nanocatalysts, an unbranched chain mechanism occurs.

During radiolysis of a suspension of nanocatalyst + H_2O and adsorbed water on the surface of nanocatalysts, water is in a liquid state. Therefore, the efficiency of hydrogen production in these processes is determined by the expression:

$$\eta = 2.96\ G(H_2) \tag{44}$$

If we take into account that the values of molecular hydrogen during the radiation-catalytic decomposition of liquid water in the presence of nano-catalysts reach $G(H_2)$=13.5 molecules/100eV values, the efficiency of the processes will be equal to:

$$\eta = 40\ \% \tag{45}$$

During thermoradiation-catalytic processes of hydrogen production, the decomposition of water occurs in a vapor state ($\Delta H = 242\ kC/mol$):

$$\eta = 2.5\ G(H_2) \tag{46}$$

Efficiency for radiation-thermocatalytic processes T = 673K with output $G(H_2) = 25.7\ molecul/100eV$:

$$\eta = 64\ \% \tag{47}$$

Thus, radiation-catalytic and radiation-thermal catalytic processes of hydrogen production in the presence of nano-catalysts ($n-ZrO_2, n-Al_2O_3$ и $n-SiO_2$) can be recommended as effective methods for converting the radiation and thermal components of nuclear-technological and energy processes (40) - (47).

Radiation-catalytic processes can be on technological radiation installations (isotope, accelerators and sources of bremsstrahlung).

Radiation-thermal catalytic processes can be implemented by a combination of radiation installations and high-temperature modular nuclear reactors. The schematic diagram of these complexes is shown in Figure 5.

At a temperature of T ≥6 73K, a high efficiency occurs during the radiation-thermocatalytic decomposition of water. The hydrogen obtained by the membrane separation from oxygen can be further used for various purposes or for the production of electricity.

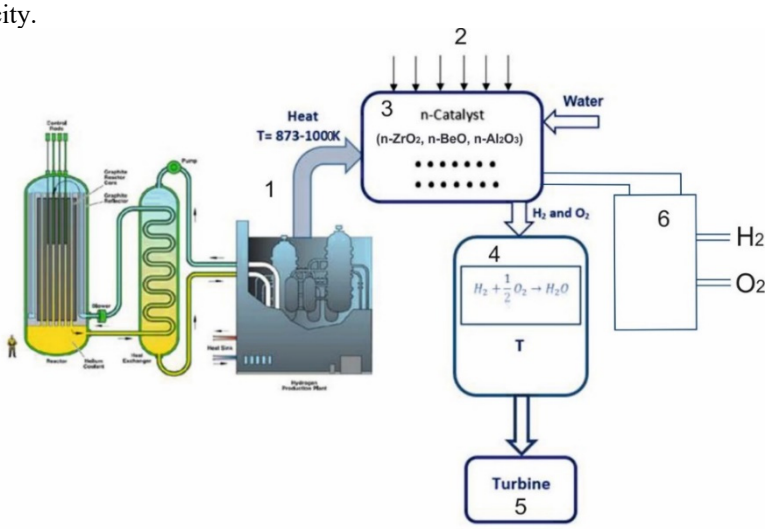

Figure 5. Scheme of the technological complex for obtaining molecular hydrogen by radiation-thermal catalytic decomposition of water with a combination of high-temperature nuclear reactors

1 - high-temperature module reactor (SMR); 2 - sources of ionizing radiation; 3 - reactor for carrying out radiation-thermal processes of hydrogen production in the presence of catalysts $n-ZrO_2, n-Al_2O_3$ и $n-BeO$); 4 - system for igniting the mixture and generating steam for the turbogenerator; 5 - turbogenerator for generating electricity; 6 - column for membrane separation of a mixture of H_2+O_2.

CONCLUSION

Based on the results obtained on the effect of the n-Si concentration in water on the yield of molecular hydrogen during water radiolysis, it can be concluded that the optimal range of n-Si concentration values for efficient conversion of ionizing radiation energy into hydrogen energy. Since at values $^{l}/_{d} \geq 3 \cdot 10^{-2}$ there is an efficient conversion of the energy of ionizing radiation into the energy of hydrogen. In order to reveal the contribution of secondary electron fluxes emitted from the solid phase in the radiation-catalytic processes of hydrogen production, the kinetics of hydrogen production processes as a result of heterogeneous decomposition of water in the presence of nano-metal (n-Zr) and individual nano-semiconductor n-Si were studied. Thus, in the case of a suspension of nano-zirconium in water, the energy of electrons emitted from the metal is completely transferred to water molecules, which leads to an increase in the yield of hydrogen. When radiolysis of water in the presence of nano-metals, energy transfer can be carried out mainly with the participation of emitted electrons. Therefore, in the case of radiolysis of water in suspension with n-Zr, the yield of hydrogen increases by 5.4 times compared to the processes of radiolysis in an adsorbed state. However, in radiation-heterogeneous processes of obtaining hydrogen from water in contact with metal systems, it is necessary to take into account that as a result of these processes surface oxidation occurs and after a certain time the systems are converted to n-Me-MeO+$H_2O_{liq.}$ systems. For nano sized oxide compounds, the mean free path of secondary electrons formed as a result of primary processes of interaction of quanta with atoms is commensurate with the particle sizes of nano-oxides (λ ≈ R_(H-oxides)). Further, these electrons interact with the electronic subsystem of silicon. For nanocatalysts, the length of free paths of secondary and subsequent generations of electrons is greater than the size of catalyst particles (R_cat≤100nm). Usually, their energy is sufficient to conduct independent radiolytic processes in the contact medium of the catalyst.

ORCID

Gunel T. Imanova, https://orcid.org/0000-0003-3275-300X

REFERENCES

[1] M. Alam, F. Miserque, M. Taguchi, and L. Boulanger, "Renanli Tuning hydrogen production during oxide irradiation through surface grofting," J. Mater Chem. **19**, 4261-4267 (2009). https://doi.org/10.1039/B901936G

[2] R. Yamada, Y. Hatano, and Z. Yoshida, "Hydrogen production of aqueous sulfuric acid solutions containing Al_2O_3, SiO_2, TiO_2 or ZrO_2 fine particles," Int. J. Hydrogen Energy, **33**, 929-936 (2008). https://doi.org/10.1016/j.ijhydene.2007.11.028
[3] S. Le Caër, "Water radiolysis: Influence of oxide surfaces on H_2 production under ionizing radiation," Water, **3**(1), 235-353 (2011). https://doi.org/10.3390/w3010235
[4] N.G. Petrik, A.B. Alexandrov, and A.I. Vall, "Interfaced energy transfer during gamma radiolysis of water on the surface of ZrO_2 and some other oxides," J. Phis. Chem. B, **105**, 5935-5944 (2001). https://doi.org/10.1021/jp004440o
[5] J.A. LaVerne, and L. Tandon, "H_2 production in the radiolysis of water on CeO_2 and ZrO_2," The Journal of Physical Chemistry B, **106**, 380-386 (2002). https://doi.org/10.1021/jp013098s
[6] J.A. LaVerne, and S.E. Tonnies, "H_2 production in the radiolysis of aqueous SiO_2. Suspensions and Slurries," The Journal of Physical Chemistry B, **107**, 7277-7280 (2003). https://doi.org/10.1021/jp0278418
[7] K. Skotnicki, and K. Bodrowski, "Molecular hydrogen formation during water radiolysis in the presence of zirconium dioxide," J. Radioanal Nucl. Chem. **304**, 473-480 (2014). https://doi.org/10.1007/s10967-014-3856-9
[8] C. Fourdrin, H. Aarrachi, C. Latrille, S. Esnouf, F. Bergaya, and S.Le. Caer, "Water Radiolysis in Excahnged-Montmorillonites: The H_2 Production Mechanisms," Environ. Sci. Technol. **47**, 9530-9537 (2013). https://doi.org/10.1021/es401490t
[9] T.N. Agayev, A.A. Garibov, G.T. Imanova, and S.Z. Melikova, "Radiation-induced heterogeneous processes of water decomposition in the presence of mixtures of silica and zirconia nanoparticles," J. High Energy Chemistry, **52**(2), 145-151 (2018). https://doi.org/10.1134/S0018143918020029
[10] I.I. Mustafayev, and H.M. Mahmudov, "Radiation-thermal desulphurization of organic fuels", J. of Radiation Researches, **2**(2), 65–70 (2015).
[11] L.Y. Jabbarova, I.I. Mustafayev, R.Y. Akbarov, and A.S. Mirzayeva, "Study of post-radiation processes in model hexane/hexene binary systems," J. of Radiation Research, **9**(1), 58–63 (2022).
[12] E.A. Carrasco-Flores, and J.A. LaVerne, "Surface species produced in the radiolysis of zirconia nanoparticles," J. Chem. Phys. **127**, 234703 (2007). https://doi.org/10.1063/1.2806164
[13] O. Roth, B. Dahlgren, and J.A. La Verne, "Radiolysis of Water on ZrO_2 Nanoparticles," J. Phys. Chem. C, **116**, 17619-17624 (2012). https://doi.org/10.1021/jp304237c
[14] A.R. Puigdollers, F. Illas, and G. Pacchioni, "Reduction of Hydrogenated ZrO_2 Nanoparticles by Water Desorption," ACS Omega, **2**, 3878-3885 (2017). https://doi.org/10.1021/acsomega.7b00799
[15] S. Le Caër, P. Rotureau, F. Brunet, T. Charpentier, G. Blain, J.P. Renault, and J.-C. Mialocq, "Radiolysis of Confined Water: Hydrogen Production at a High Dose Rate," Chem. Phys. Chem. **6**, 2585-2596 (2005). https://doi.org/10.1002/cphc.200500185
[16] J.A. LaVerne, and S.M. Pimblott, "New mechanism for H_2 formation in Water," J. Phys. Chem. B, **104**, 9820-9822 (2000). https://doi.org/10.1021/jp002893n
[17] O.D. Roth, and J.A. LaVerne, "Radiolysis of Water on ZrO_2 Nanoparticles," J. Phys. Chem. C, **116**, 17619-17624 (2012). https://doi.org/10.1021/jp304237c
[18] J. McGrady, S. Yamashita, A. Kimura, S. Kano, H. Yang, Z. Duan, T. Sato, et al., "γ-radiation effects on metal oxide particles and their wetted surfaces," Journal of Nuclear Science and Technology, 57, 463-471 (2019). https://doi.org/10.1080/00223131.2019.1691075
[19] S. Le Caër, "Water Radiolysis: Influence of Oxide Surfaces on H_2 Production under Ionizing Radiation," Water, **3**, 235-253 (2011). https://doi.org/10.3390/w3010235
[20] H. Ouerdane, B. Gervais, H. Zhou, M. Beuve, and J.-Ph. Renault, "Radiolysis of Water Confined in Porous Silica: A Simulation Study of the Physicochemical Yelds," J. Phys. Chem. C, **114**, 12667-12674 (2010). https://doi.org/10.1021/jp103127j
[21] T. Miyazaki, Y. Kuroda, and K. Marishige, "Interaction of the surface of BeO with water: in connection with the two – Deminsional Condensation of water," J. Colloid and Interface Sci. **106**(1), 154-160 (1985). https://doi.org/10.1016/0021-9797(85)90391-1
[22] A. Hofmann, S.J. Clark, M. Oppel, and I. Hahndorf, **"**Hydrogen adsorption on the tetragonal ZrO_2(101) surface: a theoretical study of an important catalytic reactant," Phys. Chem. Chem. Phys, **4**, 3500-3508 (2002). https://doi.org/10.1039/B202330J
[23] Y. Kumagai, A. Kimura, M. Taguchi, R. Nagaishi, I. Yamagishi, and T. Kimura, "Hydrogen production in gamma radiolysis of the mixture of mordenite and seawater," Journal of Nuclear Science and Technology, **50**(2), 130-138 (2013). https://doi.org/10.1080/00223131.2013.757453
[24] V F. Crumière, J. Vandenborre, R. Essehli, G. Blain, J. Barbet, and M. Fattahi, "LET effects on the hydrogen production induced by the radiolysis of pure water," Radiation Physics and Chemistry, **82**, 74-79 (2013). https://doi.org/10.1016/j.radphyschem.2012.07.010
[25] P. Rotureau, J.P. Renault, B. Lebeau, J. Patarin, and J.-C. Mialocq, "Radiolysis of Confined Water: Molecular Hydrogen Formation," Chem. Phys. Chem. **6**(7), 1316-1323 (2005). https://doi.org/10.1002/cphc.200500042
[26] M.E. Dzaugis, A.J. Spivack, and S.D. Hondt, "A quantitative model of water radiolysis and chemical production rates near radionuclide-containing solids," Radiation Physics and Chemistry, **115**, 127-134 (2015). https://doi.org/10.1016/j.radphyschem.2015.06.011
[27] J.A. LaVerne, and L. Tandon, "H_2 Production in the Radiolysis of Water on UO_2 and Other Oxides," J. Phys. Chem. B, **107**(49), 13623–13628 (2003). https://doi.org/10.1021/jp035381s
[28] S. Ismail-Beigi, and S.G. Louie, "Self-Trapped Excitons in Silicon Dioxide: Mechanism and Properties," Phys. Rev. Lett, **95**, 156401 (2005). https://doi.org/10.1103/PhysRevLett.95.156401
[29] S.C. Reiff, and J.A. LaVerne, "Radiolysis of water with aluminum oxide surfaces," J. Radiation Physics and Chemistry, **131**, 46-50 (2017). https://doi.org/10.1016/j.radphyschem.2016.10.022
[30] N.M. Dimitrijevic, A. Henglein, and D. Meisel, "Charge separation across the silica nanoparticle," Water Interface, J. Phys. Chem. B, **103**(34), 7073–7076 (1999). https://doi.org/10.1021/jp991378q
[31] T. Schatz, A.R. Cook, and D. Meisel, "Capture of charge carries at the silica nanoparticle-water interface," J. Phys. Chem. B, **103**, 10209-10219 (1999).

[32] D. Meisel, *Radiation effects in nanoparticle suspensions. Nanoscale materials*, 1st edition (Springer, Berlin, 2004).
[33] S. Isamel-Beigi, and S.G. Louie, "Self-trapped excitons in silicon-dioxide: Mechanism and Properties," Phys. Rev. Lett. **95**, 156401 (2005). https://doi.org/10.1103/PhysRevLett.95.156401
[34] V.P. Kovalev, *Secondary electrons*, (Energoatomizdat, Moscow, 1987). (in Russian)
[35] Y.D. Jafarov, S.M. Bashirova, and S.M. Aliyev, "Dependence of the yield of molecular hydrogen obtained from radiation-heterogeneous decomposition of water on particle size of silica and filling rate of particle surface of water in Si+H_2O system by the influence of gamma-quanta," Journal of Radiation Researches, **4**(2),16-23 (2017).

МЕХАНІЗМ ПРОДУКЦІЇ ВОДНЮ В ПРОЦЕСАХ РАДІАЦІЙНОГО ГЕТЕРОГЕННОГО РОЗШПИЛЕННЯ ВОДИ ЗА НАЯВНОСТЮ НАНО-МЕТАЛУ ТА НАНО-MeO

Аділь Гарібов[a], Ядігар Джафаров[a], Гюнель Іманова[a,b,c], Теймур Агаєв[a], Севіндж Баширова[d], Анар Алієв[a]
[a] Інститут радіаційних проблем Міністерства науки і освіти Азербайджанської Республіки, вул. Б. Вагабзаде, 9, AZ1143, Баку, Азербайджан
[b] Науково-дослідний центр UNEC для сталого розвитку та Creen-економіки імені Нізамі Гянджеві, Азербайджанський державний економічний університет (UNEC), вул. Істиглаліят, 6, Баку 1001, Азербайджан
[c] Хазарський університет, факультет фізики та електроніки, вул. 41 Махсаті, AZ1096, Баку, Азербайджан
[d] МІ НАСА космічних досліджень природних ресурсів, AZ 1115, Баку, С.С. Ахунзаде, 1, Азербайджан

У дослідженні визначено оптимальні значення відношення відстані між частинками до розміру частинок при радіаційно-гетерогенному радіолізі води в системах нано-Me та нано-MeO. У цих системах розглядався вплив густини води та температури системи на радіаційно-хімічне виділення молекулярного водню, отриманого при термічному та радіаційно-термічному розкладанні води. У статті також визначено вплив розмірів частинок і типу взятої проби на радіаційно-хімічний вихід молекулярного водню. У представленій статті досліджено зміну молекулярного водню залежно від адсорбованої води та каталізатора. Так, у разі суспензії наноцирконію у воді енергія електронів, що вилітають з металу, повністю передається молекулам води, що призводить до збільшення виходу водню. При радіолізі води в присутності нанометалів передача енергії може здійснюватися в основному за участю випущених електронів. Отже, при радіолізі води в суспензії з n-Zr вихід водню збільшується в 5,4 рази порівняно з процесами радіолізу в адсорбованому стані. Однак при радіаційно-гетерогенних процесах отримання водню з води, що контактує з металевими системами, необхідно враховувати, що в результаті цих процесів відбувається поверхневе окислення і через певний час системи перетворюються на n-Me-MeO+H_2O_{liq} системи. Для нанорозмірних оксидних сполук довжина вільного пробігу вторинних електронів, що утворюються в результаті первинних процесів взаємодії квантів з атомами, співмірна з розмірами частинок нанооксидів ($\lambda \approx R\_(H\text{-оксиди})$). Далі ці електрони взаємодіють з електронною підсистемою кремнію. Для нанокаталізаторів довжина вільного пробігу вторинних і наступних поколінь електронів перевищує розмір частинок каталізатора ($R\_cat \leq 100$ нм). Зазвичай їх енергії достатньо для проведення самостійних радіолітичних процесів у контактному середовищі каталізатора.

Ключові слова: *нано-Me та нано-MeO оксиди; γ-випромінювання; утворення молекулярного водню; радіоліз; друга електронна хмара*